nature materials

SUPPLEMENTARY INFORMATION

DOI: 10.1038/NMAT2930

SUPPLEMENTARY DISCUSSION

A Damage-Tolerant Glass

Marios D. Demetriou[1]*, Maximilien E. Launey[2†], Glenn Garrett[1], Joseph P. Schramm[1], Douglas C. Hofmann[1], William L. Johnson[1], and Robert O. Ritchie[2,3]

MATERIALS AND METHODS

Materials Processing

Pd-rich metal/metalloid alloys were prepared by inductively melting pure elements in quartz tubes under inert atmosphere. Alloy ingots were fluxed with B_2O_3 at ~1200 K for ~1000 s. Glass formation was achieved by melting fluxed ingots in quartz tubes with 0.5-mm-thick walls and rapidly water-quenching. The quartz-tube water quenching method was found to be more efficient in terms of glass formation than copper-mold casting. When water-quenched from the molten state in a 0.5-mm-thick wall quartz tube, alloy $Pd_{79}Ag_{3.5}P_6Si_{9.5}Ge_2$ is found capable of forming glassy rods 6 mm in diameter.

Mechanical Characterization

Amorphous tensile-test specimens were produced by water-quenching round tensile-bar shaped quartz tubes containing the molten alloy. Tensile tests of glassy $Pd_{79}Ag_{3.5}P_6Si_{9.5}Ge_2$ were performed at room temperature. The specimen gauge sections were 1.5 mm in diameter and 20 mm in length. Tests were performed at a strain rate of 5×10^{-4} s^{-1} on a screw-driven Instron testing machine (Instron, Norwood, MA), and strain was recorded using an Epsilon extensometer.

Rectangular beams for flexure measurements were prepared by grounding 3-mm diameter amorphous rods. The beam specimens had thickness, *B*, of 2.1 mm, width, *W*, of 2.1 mm and length, *L*, 20 mm. Fracture toughness resistance-curve (R-curve) measurements were performed on single-edge notched beam, SE(B), specimens loaded

[1] Keck Engineering Laboratories, California Institute of Technology, Pasadena, CA 91125, USA
[2] Materials Sciences Division, Lawrence Berkeley National Laboratory, Berkeley, CA 94720, USA
[3] Department of Materials Science and Engineering, University of California, Berkeley, CA 94720, USA
* To whom correspondence should be addressed. Email: marios@caltech.edu
†Present address: Cordis Corporation, a Johnson & Johnson Company, 6500 Paseo Padre Parkway, Fremont, CA 94555, USA

DOI: 10.1038/NMAT2930

in three-point bending with a support span of 15 mm. The notches were first introduced using a low-speed diamond saw, and then sharpened using a razor-micro-notching technique. Micro-notches, with a root radius of 5-10 μm were obtained by repeatedly sliding a razor blade over the saw-cut notch using a custom-made rig, while continually irrigating with a 1 μm diamond slurry. Micro-notches resembling sharp cracks with initial crack length, a, of ~ 1.0 mm, were generated in general accordance with ASTM standards[S1]. Prior to testing, specimens were polished to a 1 μm diamond suspension surface finish on both faces.

Nonlinear-elastic fracture mechanics methods were used to evaluate the fracture toughness, which involve resistance-curve characterization in terms of the J-integral. Of particular importance here are the specific validity criteria in terms of the size of the test sample and the length of the pre-crack (see ASTM Standard E-1820[S1]). This is because the crack-tip fields are invariably described by asymptotic solutions defined in terms of one prevailing mode of deformation (*e.g.*, linear elasticity, nonlinear elasticity, etc.), and regions that do not conform to this deformation mode (*e.g.*, the plastic zone in a linear-elastic K-field) must be small enough to ignore, thereby placing restrictions on the minimum specimen size relative to the crack size. For a linear-elastic K_{Ic} measurement, the crack-tip plastic-zone size must be typically an order of magnitude smaller than (i) the in-plane dimensions of crack length a and remaining uncracked ligament b (small-scale yielding condition), and (ii) the out-of-plane thickness dimension B (a condition of plane strain); *i.e.*, $a, b, B \geq 2.5 (K_c/\sigma_y)^2$, where σ_y is the yield strength. For example, for a K_c value of 200 MPa.m$^{1/2}$ and σ_y value of 1500 MPa, this leads to specimen size requirements such as $a, b, B \geq 45$ mm. For nonlinear elastic J measurements, similar validity criteria exist although the size requirements are much less restrictive; specifically $b, B \geq 10 (J_c/\sigma_y)$. For example, for a J_c value of 450 kJ/m^2 and σ_y value of 1500 MPa, this leads to $b, B \geq 3$ mm.

To further relax the size constraints such that even smaller bend bars can be tested (*i.e.*, to overcome the size constraints for meeting the small-scale yielding conditions) while still properly accounting for the extension of the crack, we here implemented a crack-tip opening displacement (CTOD) approach. This is a nonlinear-elastic fracture mechanics methodology where measurements of CTOD, δ_t, can be related to the J-integral by[S2]:

$$J = d_n \sigma_o \delta_t \qquad \text{(S1)}$$

where σ_o is defined as the flow stress (the average of the yield and ultimate stresses), and d_n is a constant tabulated from the strain-hardening exponent, n, of the material[S2].

Upon yielding, it is well established that metallic glasses locally (*i.e.*, within an operating shear band) strain-soften. Consequently, when subject to pure tension, where the glass typically fails along a single shear band by unconstrained slipping, no global

strain hardening is generally detectable. However, when subject to a quasi-stable loading geometry like bending, where the glass is under tension on one side of the neutral axis and under compression on the other, generation and proliferation of multiple shear bands is possible (depending on the toughness of the glass), occurring predominantly on the compression side. The intersection and multiplication of shear bands generally gives rise to compatibility stresses between deformed and undeformed regions, which typically induce a small apparent global hardening effect detectable in the true stress-stain response. For the toughness measurements, this limited degree of strain hardening occurring at the continuum scale is essentially sufficient to ensure "CTOD dominance" at the crack tip.

Here, the hardening exponent n associated with subjection the $Pd_{79}Ag_{3.5}P_6Si_{9.5}Ge_2$ glass in bending was determined using a three-point bending test on an unnotched 2.1 mm × 2.1 mm specimen. The test was performed over a support span of 15 mm on a servo-hydraulic testing machine (MTS, Eden Prairie, MN) at a displacement rate of 10 μm/s (Supplementary Figures 1 & 2). As such, quantitative stress-strain information is generated that specifically reflects the loading conditions of the fracture toughness test.

In the fracture toughness test, δ-Δa R-curves were measured on three micro-notched specimens *in situ* in a Hitachi S-4300SE/N ESEM (Hitachi America, Pleasanton, CA) using a Gatan Microtest three-point bending stage (Gatan, Abington, UK). The crosshead displacement was measured with a linear variable displacement transducer, while the load was recorded using a 2000 N load cell. The CTOD and crack extension were monitored at regular intervals in secondary electron mode *in vacuo* (10^{-4} Pa) at a 20 kV excitation voltage. The crack-tip opening displacement, δ_t, was measured graphically as the opening distance between the intercept of two 45°-lines drawn back from the tip with the deformed profile (Fig. S1), as derived by Shih[S2] from the Hutchinson-Rice-Rosengren (HRR) singularity[S2-5]. At each interval i, δ_t is defined as:

$$\delta_t = \delta_i - \delta_0, \tag{S2}$$

where δ_i is the actual crack-tip opening displacement and δ_0 is the initial crack-tip opening displacement before loading. J values were then calculated using Eq. (S1) for each crack increment and converted to equivalent K values through the J-K equivalence relationship for nominally mode I fracture in plane stress:

$$K_J = (JE)^{1/2}, \tag{S3}$$

with E = 88 GPa the Young's modulus of the $Pd_{79}Ag_{3.5}P_6Si_{9.5}Ge_2$ glass.

DOI: 10.1038/NMAT2930

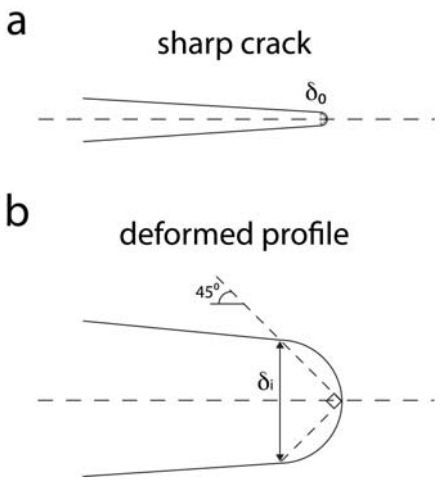

Figure S1: Procedure for defining the crack-tip opening displacement. (**a**) Sharp crack and (**b**) deformed crack profile illustrating the 45° procedure for CTOD.

It's important to note that Eq. (S1) is valid for both plane strain and plane stress conditions, and as long as the HRR fields dominate. In the large-scale yielding regime (as in the present case), the size of the region dominated by the singularity fields is dependent on specimen geometry[S3]; in this regime, Shih[S2] shows that the relationship between J and δ_t, as expressed in Eq. (S1), holds under large-scale plasticity for a hardening material when the uncracked ligament is subjected primarily to bending.

To verify this CTOD approach on a glassy material with a well-known toughness, we compared the estimated K_J against the value obtained using direct J-integral measurements. However, unlike the glass presented here, most monolithic metallic glasses in bulk dimensions do not exhibit rising R-curves (*i.e.*, they fail catastrophically soon after yielding by unstable crack extension), thus the full extent of the method cannot be assessed. Instead, the method was implemented on a ductile-phase-reinforced metallic glass ($Zr_{39.6}Ti_{33.9}Nb_{7.6}Cu_{6.4}Be_{12.5}$)[S6], where the extended R-curve is well documented[S7]. As shown in Supplementary Figure 3, good agreement was obtained between the two methods, but most importantly, the CTOD method is shown to provide a *conservative* estimate of the toughness (*i.e.*, it slightly underestimates the toughness).

Toughness correlation

A scaling law is proposed in this work by which the plastic zone radius of a metallic glass is correlated to the plastic shearing enabled within a shear band prior to nucleating a cavity that will initiate a crack. Specifically, the plastic zone radius, $r_p = K_c/\pi\sigma_y^2$, is correlated to the number of activated shear events enabled prior to the activation of a cavitation event, denoted here by f:

$$\log\left(\frac{K_c^{\,2}}{\pi\sigma_y^2}\right) \sim \log(f) \approx \frac{T_g}{T}\left(\frac{B}{G}-1\right) \qquad \text{(S4)}$$

In the above expression, T_g is the glass transition temperature, T is a reference temperature (here taken to be the test temperature, *i.e.*, T = 300 K), G the shear modulus, and B the bulk modulus. Data for ten metallic glass alloys are utilized, listed in Table S1 below. A plot of the scaling law, Eq. (S4), for the ten systems is presented in Fig. 4c of the main article.

Glass-Forming Alloy	G [GPa]	B [GPa]	T_g [K]	σ_y [MPa]	K_c [MPa.m$^{1/2}$]	References
$Mg_{65}Cu_{25}Tb_{10}$	19.6	44.71	415	660	2	S8,S9
$La_{55}Al_{25}Ni_5Cu_{10}Co_5$	15.6	44.2	430	700	5	S8,S10,S11
$Fe_{58}Co_{6.5}Mo_{14}C_{15}B_6Er_{0.5}$	74.0	177.0	790	3700	26.5	S12,S13
$Fe_{66}Cr_3Mo_{10}C_{10}B_3P_8$	66.5	172.0	721	3100	39.3	S12,S14
$Fe_{70}Ni_5Mo_5C_5B_{2.5}P_{12.5}$	57.3	150.1	696	2670	49.8	S15
$Zr_{55}Cu_{30}Ni_5Al_{10}$	34.7	117.9	684	1650	43.3	S16-18
$Zr_{41.2}Ti_{13.8}Cu_{12.5}Ni_{10}Be_{22.5}$	34.1	114.1	618	1850	55	S8,S19
$Cu_{60}Zr_{20}Hf_{10}Ti_{10}$	36.9	128.2	754	1950	67.6	S20
$Pt_{57.5}Cu_{14.7}Ni_{5.3}P_{22.5}$	33.3	198.7	508	1400	81.5	S21
$Pd_{79}Ag_{3.5}P_6Si_{9.5}Ge_2$	31.1	171.6	613	1490	203	Present

Table S1: Data for ten metallic glass systems used in the correlation given by Eq. (S4).

Supplementary References

S1. ASTM E1820-08, *Annual Book of ASTM Standards, Vol. 03.01: Metals - Mechanical Testing; Elevated and Low-temperature Tests; Metallography* (ASTM International, West Conshohocken, Pennsylvania, USA, 2008).

S2. Shih, C. F. Relationships between the J-Integral and the Crack Opening Displacement for Stationary and Extending Cracks. *J. Mech. Phys. Solids* 29, 305-326 (1981).

S3. Shih, C. F. & German, M. D. Requirements for a One-Parameter Characterization of Crack Tip Fields by the HRR Singularity. *Int. J. Fract.* 17, 27-43 (1981).

S4. Hutchinson, J. W. Plastic Stress and Strain Fields at a Crack Tip. *J. Mech. Phys. Solids* 16, 337-342 (1968).

S5. Rice, J. R. & Rosengren, G. F. Plane Strain Deformation near a Crack Tip in a Power-Law Hardening Material. *J. Mech. Phys. Solids* 16, 1-12 (1968).

S6. Hofmann, D. C. *et al.* Designing Metallic Glass Matrix Composites with High Toughness and Tensile Ductility. *Nature* 451, 1085-U3 (2008).

S7. Launey, M. E. *et al.* Fracture Toughness and Crack Resistance Curve Behavior in Metallic Glass Matrix Composites. *Appl. Phys. Lett.* 94, 241910 (2009).

DOI: 10.1038/NMAT2930

S8. Xi, X. K. *et al.* Fracture of Brittle Metallic Glasses: Brittleness or Plasticity. *Phys. Rev. Lett.* 94, 125510 (2005)

S9. Xi, X. K. *et al.* Highly Processable $Mg_{65}Cu_{25}Tb_{10}$ Metallic Glass. *J. Non-Cryst. Sol.* 344, 189-192 (2004).

S10. Johnson, W. L. & Samwer, K. A Universal Criterion for Plastic Yielding of Metallic Glasses with a $(T/T_g)^{2/3}$ Temperature Dependence. *Phys Rev. Lett.* 95, 195501 (2005).

S11. Nagendra, N. *et al.* Effect of Crystallinity on the Impact Toughness of a La-based Bulk Metallic Glass. *Acta Mater.* 48, 2603-2615 (2000).

S12. Nouri, A. S. *et al.* Chemistry (Intrinsic) and Inclusion (Extrinsic) Effects on the Toughness and Weibull Modulus of Fe-based Bulk Metallic Glasses. *Phil. Mag. Lett.* 88, 853-861 (2008).

S13. Gu, X. J. & Poon, S. J. Mechanical Properties of Iron-Based bulk Metallic Glasses. *J. Mater. Res.* 22, 344-351 (2007).

S14. Gu, X. J. *et al.* Mechanical Properties, Glass Transition Temperature, and Bond Enthalpy Trends of High Metalloid Fe-Based Bulk Metallic Glasses. *Appl. Phys. Lett.* 92, 161910 (2008).

S15. Demetriou, M. D. *et al.* Glassy Steel Optimized for Glass-Forming Ability and Toughness. *Appl. Phys. Lett.* 92, 161910 (2008).

S16. Kawashima, A. *et al.* Fracture toughness of $Zr_{55}Cu_{30}Al_{10}Ni_5$ Bulk Metallic Glass by 3-Point Bend Testing. *Mater. Trans.* 46, 1725-1732 (2005).

S17. Luo, J. *et al.* Effects of Yttrium and Erbium Additions on Glass Forming Ability and Mechanical Properties of Bulk Glassy Zr-Al-Ni-Cu Alloys. *Mater. Trans.* 47, 450-453 (2006).

S18. Vaillant, M. L. et al. Changes in the Mechanical Properties of a $Zr_{55}Cu_{30}Al_{10}Ni_5$ Bulk Metallic Glass due to Heat Treatments Below 540 °C. *Scripta Mater.* 47, 19-23 (2002).

S19. Gilbert, C. J. *et al.* Fracture Toughness and Fatigue Crack Propagation in a Zr-Ti-Ni-Cu-Be Bulk Metallic Glass. *Appl. Phys. Lett.* 71, 476-478 (1997).

S20. Wesseling, P. *et al.* Preliminary Assessment of Flow, Notch Toughness, and High-Temperature Behavior of $Cu_{60}Zr_{20}Hf_{10}Ti_{10}$ Bulk Metallic Glass. *Scripta Mater.* 51, 151-154 (2004).

S21. Schroers, J. & Johnson, W. L. Ductile bulk metallic glass. *Phys. Rev. Lett.* 93, 255506 (2004).

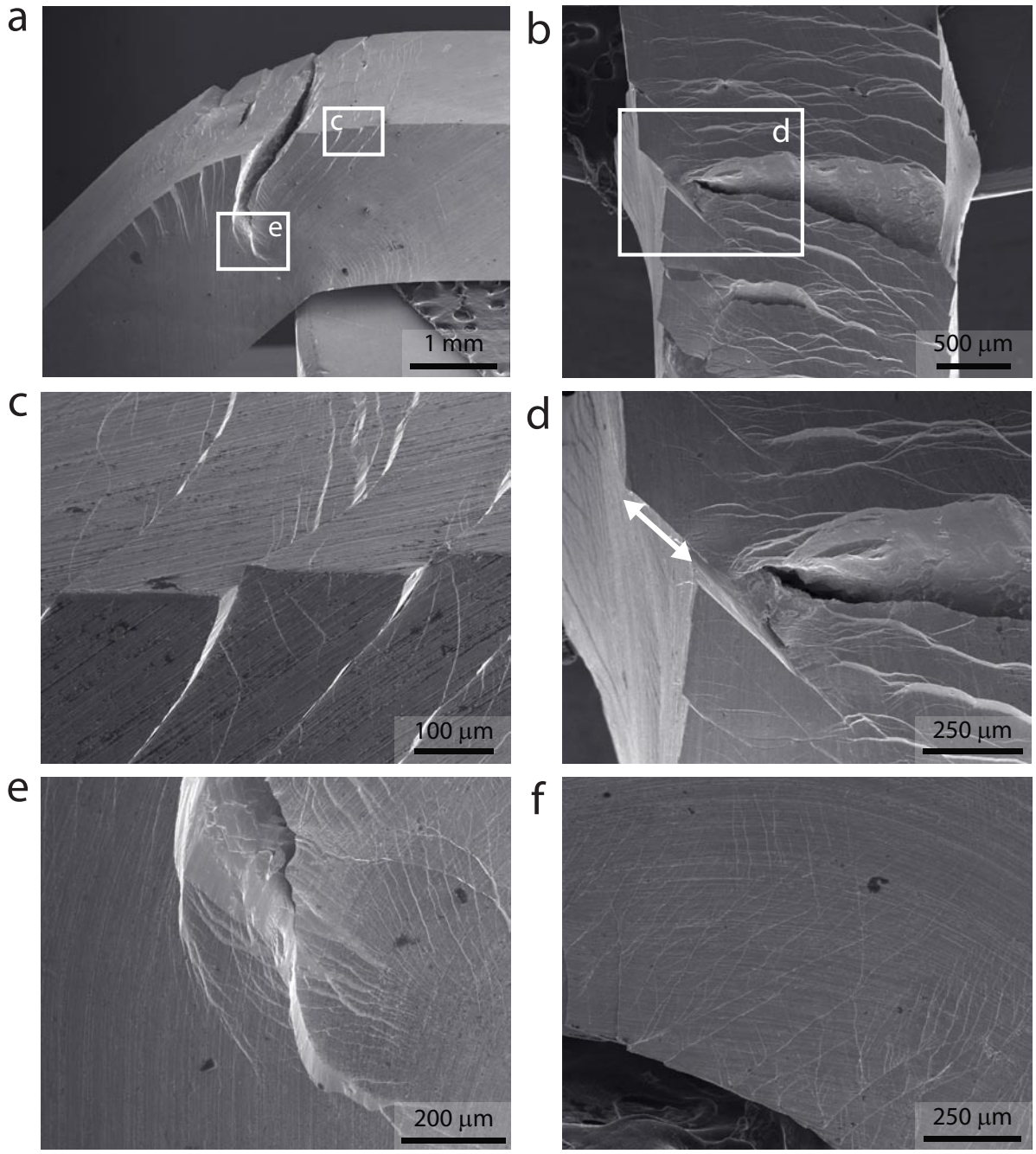

Supplementary Figure 1: Secondary electron micrographs taken after a three-point bending test on an unnotched $Pd_{79}Ag_{3.5}P_6Si_{9.5}Ge_2$ glassy specimen. (a, b) A dense network of shear bands is observed in the tension side of the specimen along with an open crack that propagated in a stable fashion towards the center of the beam. The sample did not fracture catastrophically after undergoing the entire bending strain applicable by the fixture; (c, d) Shear offsets in the tension side are shown, that appear to be as long as 200 μm (see arrow in d). (e) Plastic-flow stabilization at the crack tip promoting stable crack growth, and (f) plastic flow in the compression side.

DOI: 10.1038/NMAT2930

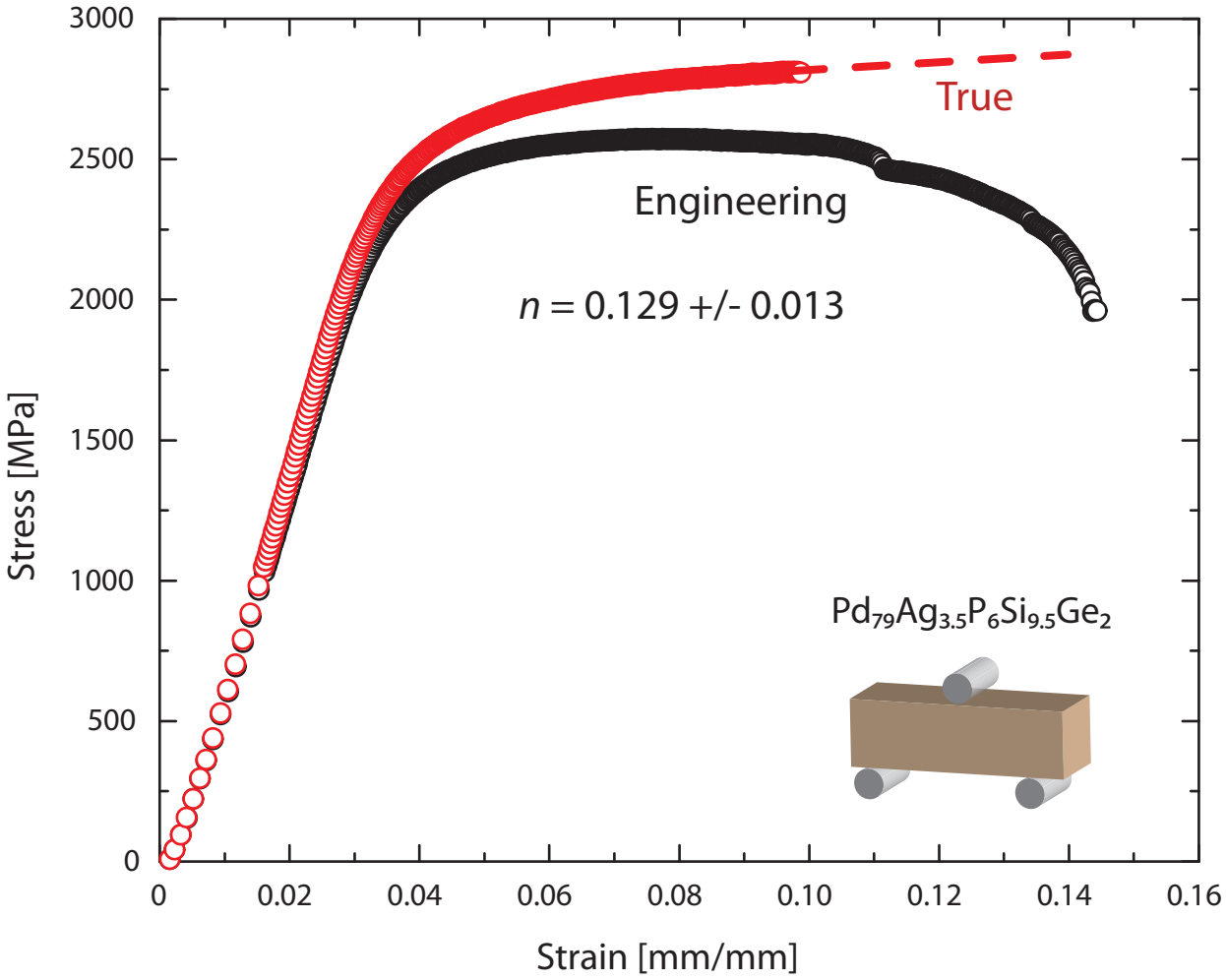

Supplementary Figure 2: Engineering and true stress-strain curve for an unnotched $Pd_{79}Ag_{3.5}P_6Si_{9.5}Ge_2$ glassy specimen tested in a three-point bending configuration. The serration at ~11% strain (engineering curve) marks the development of the crack seen in Supplementary Figure 1, and the decreasing loading response following the serration reflects the loss of rigidity due to crack extension. The sample did not fracture catastrophically after undergoing 14% bending strain (see Supplementary Figure 1). A slight hardening response is evident in the true stress-strain curve, which can be attributed to multiplication and intersection of shear bands giving rise to local compatibility stresses. The strain-hardening exponent, n, was measured using the relationship: $\sigma_T = C\varepsilon_T^n$, where σ_T and ε_T are, respectively, the true stress and strain, and C is a constant.

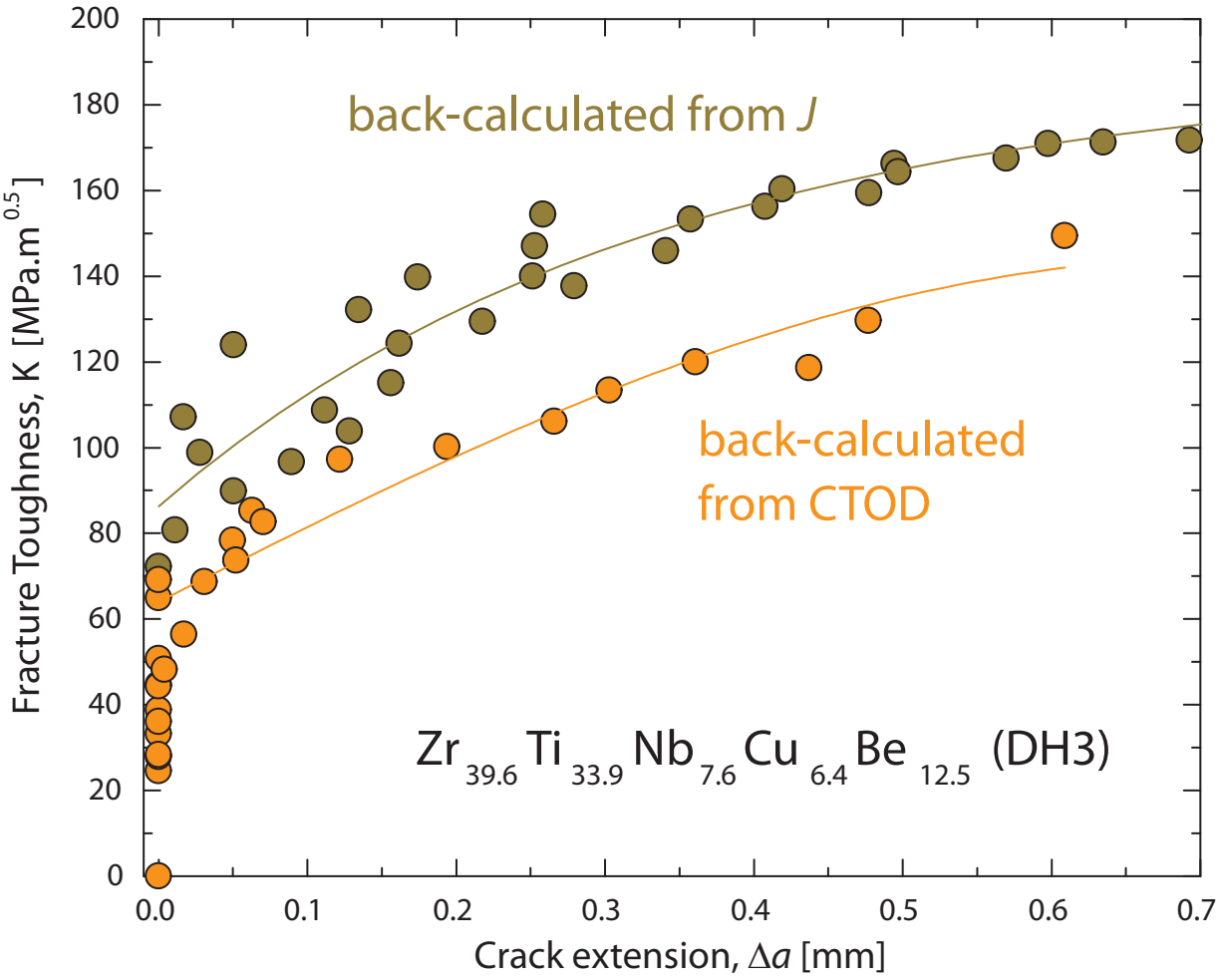

Supplementary Figure 3: Comparison of R-curves derived using direct *J*-integral and CTOD methods for ductile-phase-reinforced metallic glass $Zr_{39.3}Ti_{33.9}Nb_{7.6}Cu_{6.4}Be_{12.5}$. Good agreement between the two measurements techniques is shown. The CTOD approach utilized in the present work can be seen to provide a somewhat conservative estimate of the fracture toughness.